Burn Control in Fusion Reactors Using Simultaneous Boundary and Distributed Actuation

Mark D. Boyer and Eugenio Schuster

***Abstract*— The control of the plasma density and temperature profiles is one of the fundamental problems in nuclear fusion reactors. During reactor operation, the spatial profiles of deuterium-tritium fuel, alpha particles generated by fusion reactions, and energy must be precisely regulated. In this work we combine distributed actuation with a backstepping boundary control law to stabilize an unstable equilibrium in a burning plasma. Disturbance estimation update laws are included to improve disturbance rejection and tracking. A one-dimensional approximation of the transport equation for energy, as well as for the densities of deuterium-tritium fuel ions and alpha particles, is represented in cylindrical coordinates by a system of partial differential equations (PDEs). The PDE system is discretized in space using a finite difference method and a backstepping design is applied to obtain a discrete transformation from the original system into a particular target system chosen to facilitate the use of additional actuators distributed throughout the plasma. Numerical simulations show that a controller designed on a very coarse grid can stabilize the system and that distributed actuation improves the system response.**

I. Introduction

For nuclear fusion to become an economical means of producing energy, tokamak reactors will have to operate at high fusion gain (the ratio of power produced to power required to sustain a discharge) for extended durations, ideally reaching steady state. In present-day experiments, much work is being done to identify operating scenarios that could lead to steady-state operation and reduced reactor size and cost. However, precise feedback control over plasma parameters, including the magnitudes and spatial distributions of kinetic variables (e.g., plasma density, temperature, and current), may be required to achieve and maintain these scenarios. Furthermore, in burning plasmas, for which the dominant source of heating needed to sustain the plasma is from fusion, the task of regulating operating conditions will be complicated by the nonlinear coupling of fusion power with the dynamics of density and temperature, and by a potential thermal instability.

Most approaches to the control of kinetic variables in tokamaks begin by considering 0-D (zero-dimensional) models of transport in which the system equations are averaged over the volume of the plasma. This allows the problem to be approached with lumped-parameter control design techniques. The resulting nonlinear model is often simplified further by linearizing the system around a particular operating point, enabling the use of standard linear control techniques. In [1], [2], [3], the linearization of the model was avoided, and nonlinear and adaptive control techniques were used to achieve much higher levels of performance and robustness. However, these 0-D control efforts do not take into account the 1-D (one-dimensional) effect of modulating the bulk heating, fueling, and impurity injection on the shape of the spatial profiles. In a reactor, the heating and fueling rates are indeed distributed throughout the plasma and affect the shape of the kinetic profiles, which in turn affects confinement, magnetohydrodynamic stability, and reactor performance.

The importance of controlling kinetic profiles in burning plasmas has been recognized in previous work, including, [4], [5], [6], [7], and [8]. In these pieces of work, a 1-D plasma model is represented by a set of partial differential equations (PDEs) and various methods are utilized to reduce the distributed parameter model to a lumped-parameter one. The resulting set of ODEs are then linearized and conventional linear control techniques are used for controller design. Through a backstepping boundary feedback technique, the control methods presented in [9], [10] avoided linearization, stabilizing density and temperature profiles in non-burning and burning plasmas, respectively. The backstepping approach avoids the operating limits created by linearization. In this work, we extend the approach to include both boundary and distributed actuation, and to include online disturbance estimation, improving system response, disturbance rejection, and tracking performance.

The paper is organized as follows. In Section II a one-dimensional burning plasma model is introduced. The control objective and controller design are outlined in Section III and Section IV, respectively. Simulation results showing successful stabilization of an unstable set of equilibrium profiles are contained in Section V. Concluding remarks and a discussion of future work are given in Section VI.

II. One-Dimensional Burning Plasma Model

The model used in this work includes the dynamics of the density of α-particles, deuterium-tritium fuel, and stored energy, and is based on standard 1-D transport equations. To simplify presentation, we consider a constant diffusivity and a negligible pinch velocity, however, the control approach could be extended to account for these effects, as done in [9]. The particle densities and energy are governed by:

$$\frac{\partial n_\alpha}{\partial t} = \frac{1}{r}\frac{\partial}{\partial r} r\left(D\frac{\partial n_\alpha}{\partial r}\right) + \left(\frac{n_{DT}}{2}\right)^2 \langle \sigma v \rangle \tag{1}$$

$$\frac{\partial n_{DT}}{\partial t} = \frac{1}{r}\frac{\partial}{\partial r} r\left(D\frac{\partial n_{DT}}{\partial r}\right) - 2\left(\frac{n_{DT}}{2}\right)^2 \langle \sigma v \rangle + S_{DT} \tag{2}$$

This work was supported by the NSF CAREER award program (ECCS-0645086). M. D. Boyer (mdb209@lehigh.edu), and E. Schuster are with the Department of Mechanical Engineering and Mechanics, Lehigh University, Bethlehem, PA 18015, USA.

$$\frac{\partial E}{\partial t} = \frac{1}{r}\frac{\partial}{\partial r} r\left(D\frac{\partial E}{\partial r}\right) + Q_\alpha \left(\frac{n_{DT}}{2}\right)^2 \langle \sigma v \rangle - P_{rad} + P_{aux} \quad (3)$$

where $\langle \sigma v \rangle$ is the DT reactivity, S_{DT} is the distributed DT fuel injection, and $Q_\alpha = 3.52$ MeV is the alpha particle energy. P_{aux} and P_{rad} represent the distributed auxiliary power and radiation losses, respectively. We consider distributed actuators of the form $S_{DT} = u_{fuel}(t)\hat{S}_{DT}(r)$, $P_{aux} = u_{aux}(t)\hat{P}_{aux}(r)$, i.e., fixed spatial deposition profiles $\hat{S}_{DT}(r)$ and $\hat{P}_{aux}(r)$ and controllable magnitudes $u_{fuel}(t)$ and $u_{aux}(t)$. Deposition profiles used in this work are shown in Figure 1.

The DT reactivity $\langle \sigma v \rangle = exp\left(\frac{a_1}{T^r} + a_2 + a_3 T + a_4 T^2 + a_5 T^3 + a_6 T^4\right)$ is a highly nonlinear, positive, and bounded function of the plasma temperature T [11]. The plasma temperature is a function of the energy and total plasma density, i.e., $T = \frac{2}{3}\frac{E}{n}$, and the total plasma density is given by the sum of ion and electron densities, $n_i = n_{DT} + n_\alpha$ and $n_e = n_{DT} + 2n_\alpha$, i.e., $n = 2n_{DT} + 3n_\alpha$. The radiation loss P_{rad} considered in this work is given by $P_{rad} = P_{brem} = A_b Z_{eff} n_e^2 \sqrt{T}$. where $A_b = 5.5 \times 10^{-37}$ $\mathrm{Wm}^3/\sqrt{\mathrm{keV}}$ is the bremsstrahlung radiation coefficient, $Z_{eff} = \sum_i \frac{n_i Z_i^2}{n_e} = \frac{n_{DT}+4n_\alpha}{n_e}$ is the effective atomic number, and n_e is the electron density. Note that the control design presented in this work could easily be extended to include other forms of radiation losses and this choice of model is only used for simplification of presentation.

The boundary conditions are given by

$$\left.\frac{\partial n_\alpha}{\partial r}\right|_{r=0} = \left.\frac{\partial n_{DT}}{\partial r}\right|_{r=0} = \left.\frac{\partial E}{\partial r}\right|_{r=0} = 0, \quad (4)$$

$$n_\alpha(a) = u_\alpha(t), \quad n_{DT}(a) = u_{DT}(t), \quad E(a) = u_E(t), \quad (5)$$

where $u_\alpha(t)$, $u_{DT}(t)$, and $u_E(t)$ are considered actuators.

III. Control Objective

At equilibrium, the model simplifies to a set of ODEs with respect to the space coordinate, i.e.,

$$0 = \frac{1}{r}\frac{\partial}{\partial r} r\left(D\frac{\partial \bar{n}_\alpha}{\partial r}\right) + \bar{S}_\alpha \quad (6)$$

$$0 = \frac{1}{r}\frac{\partial}{\partial r} r\left(D\frac{\partial \bar{n}_{DT}}{\partial r}\right) - 2\bar{S}_\alpha + \bar{u}_{fuel}\hat{S}_{DT} \quad (7)$$

$$0 = \frac{1}{r}\frac{\partial}{\partial r} r\left(D\frac{\partial \bar{E}}{\partial r}\right) + Q_\alpha \bar{S}_\alpha - \bar{P}_{rad} + \bar{u}_{aux}\hat{P}_{aux} \quad (8)$$

where we have written the alpha particle generation as $S_\alpha = \left(\frac{n_{DT}}{2}\right)^2 \langle \sigma v \rangle$ and we use upper bar notation to represent the equilibrium value of a variable. The equilibrium profiles are determined by the equilibrium fueling $\bar{u}_{fuel}$, heating $\bar{u}_{aux}$, and boundary conditions $\bar{u}_\alpha$, $\bar{u}_{DT}$, and $\bar{u}_E$.

We consider perturbations in the profiles, i.e., $n_\alpha(r,t) = \bar{n}_\alpha(r) + \tilde{n}_\alpha(r,t)$, $n_{DT}(r,t) = \bar{n}_{DT}(r) + \tilde{n}_{DT}(r,t)$, $E(r,t) = \bar{E}(r) + \tilde{E}(r,t)$, $S_\alpha(r,t) = \bar{S}_\alpha(r) + \tilde{S}_\alpha(r,t)$, and $P_{rad}(r,t) = \bar{P}_{rad}(r) + \tilde{P}_{rad}(r,t)$, and the presence of distributed feedback $(\tilde{u}_{fuel}, \tilde{u}_{aux})$ and constant input disturbances (d_{fuel}, d_{aux}), i.e.,

$$S_{DT}(r,t) = \left(\bar{u}_{fuel} + \tilde{u}_{fuel} + d_{fuel}\right)\hat{S}_{DT}(r)$$

$$P_{aux}(r,t) = \left(\bar{u}_{aux} + \tilde{u}_{aux} + d_{aux}\right)\hat{P}_{aux}(r)$$

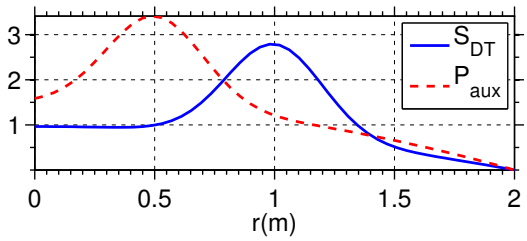

Fig. 1: Distributed actuator deposition profiles used in this work.

We also consider boundary feedback $(\tilde{u}_\alpha, \tilde{u}_{DT}, \tilde{u}_E)$ and constant boundary disturbances (d_α, d_{DT}, d_E). We first attempt to cancel the effect of the unknown disturbances by defining the feedback laws $\tilde{u}_\alpha = v_\alpha - \hat{d}_\alpha$, $\tilde{u}_{DT} = v_{DT} - \hat{d}_{DT}$, $\tilde{u}_E = v_E - \hat{d}_E$, $\tilde{u}_{fuel} = v_{fuel} - \hat{d}_{fuel}$, $\tilde{u}_{aux} = v_{aux} - \hat{d}_{aux}$, where v_α, v_{DT}, v_E, v_{fuel}, and v_{aux} are inputs to be defined later, and $\hat{d}_\alpha$, $\hat{d}_{DT}$, $\hat{d}_E$, $\hat{d}_{fuel}$, and $\hat{d}_{aux}$ are estimates of the disturbances, which will be obtained from update laws, also to be defined later. We define the disturbance estimation errors $\tilde{d}_\alpha = d_\alpha - \hat{d}_\alpha$, $\tilde{d}_{DT} = d_{DT} - \hat{d}_{DT}$, $\tilde{d}_E = d_E - \hat{d}_E$, $\tilde{d}_{fuel} = d_{fuel} - \hat{d}_{fuel}$, and $\tilde{d}_{aux} = d_{aux} - \hat{d}_{aux}$. By substituting (6), (7), and (8) into (1), (2), and (3), the dynamics of the deviation variables $\tilde{n}_\alpha(r,t)$, $\tilde{n}_{DT}(r,t)$, and $\tilde{E}(r,t)$ can be written as

$$\frac{\partial \tilde{n}_\alpha}{\partial t} = D\frac{\partial^2 \tilde{n}_\alpha}{\partial r^2} + \frac{1}{r}D\frac{\partial \tilde{n}_\alpha}{\partial r} + \tilde{S}_\alpha \quad (9)$$

$$\frac{\partial \tilde{n}_{DT}}{\partial t} = D\frac{\partial^2 \tilde{n}_{DT}}{\partial r^2} + \frac{1}{r}D\frac{\partial \tilde{n}_{DT}}{\partial r} - 2\tilde{S}_\alpha + \left(v_{fuel} + \tilde{d}_{DT}\right)\hat{S}_{DT} \quad (10)$$

$$\frac{\partial \tilde{E}}{\partial t} = D\frac{\partial^2 \tilde{E}}{\partial r^2} + \frac{1}{r}D\frac{\partial \tilde{E}}{\partial r} + Q_\alpha \tilde{S}_\alpha - \tilde{P}_{rad} + \left(v_{aux} + \tilde{d}_{aux}\right)\hat{P}_{aux} \quad (11)$$

The boundary conditions are written as

$$\left.\frac{\partial \tilde{n}_\alpha}{\partial r}\right|_{r=0} = \left.\frac{\partial \tilde{n}_{DT}}{\partial r}\right|_{r=0} = \left.\frac{\partial \tilde{E}}{\partial r}\right|_{r=0} = 0, \quad (12)$$

$$\tilde{n}_\alpha(a) = v_\alpha(t) + \tilde{d}_\alpha, \quad \tilde{n}_{DT}(a) = v_{DT}(t) + \tilde{d}_{DT},$$
$$\tilde{E}(a) = v_E(t) + \tilde{d}_E. \quad (13)$$

The objective of the controller is to force $\tilde{n}_\alpha(r,t)$, $\tilde{n}_{DT}(r,t)$ and $\tilde{E}(r,t)$ to zero using distributed actuators v_{fuel} and v_{aux}, and boundary actuators v_α, v_{DT}, and v_E, while accounting for the effect of disturbance estimation errors.

IV. Controller Design

A backstepping technique is used to transform the original system of equations into a particular target system. The target system is rendered asymptotically stable through the choice of boundary conditions, distributed actuator control laws, and update laws for the disturbance estimations. Figure 2 illustrates the approach. By defining $h = \frac{1}{N}$, where N is an integer, and using the notation $x^i(t) = x(ih,t)$, $i = 0,1,...,N$, the discretized version of (9) - (11) can be written as

$$\dot{\tilde{n}}^i_\alpha = D\frac{\tilde{n}^{i+1}_\alpha - 2\tilde{n}^i_\alpha + \tilde{n}^{i-1}_\alpha}{h^2} + \frac{D}{ih}\frac{\tilde{n}^{i+1}_\alpha - \tilde{n}^i_\alpha}{h} + \tilde{S}^i_\alpha \quad (14)$$

$$\dot{\tilde{n}}^i_{DT} = D\frac{\tilde{n}^{i+1}_{DT} - 2\tilde{n}^i_{DT} + \tilde{n}^{i-1}_{DT}}{h^2} + \frac{D}{ih}\frac{\tilde{n}^{i+1}_{DT} - \tilde{n}^i_{DT}}{h} - 2\tilde{S}^i_\alpha + \left(v_{fuel} + \tilde{d}_{fuel}\right)\hat{S}^i_{DT} \quad (15)$$

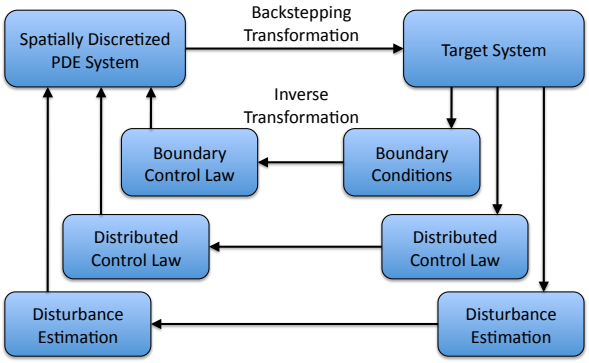

Fig. 2: Schematic of the backstepping control design.

$$\dot{\tilde{E}}^i = D\frac{\tilde{E}^{i+1}-2\tilde{E}^i+\tilde{E}^{i-1}}{h^2}+\frac{D}{ih}\frac{\tilde{E}^{i+1}-\tilde{E}^i}{h} +Q_\alpha\tilde{S}^i_\alpha-\tilde{P}^i_{rad}+\left(v_{aux}+\tilde{d}_{aux}\right)\hat{P}^i_{aux} \tag{16}$$

with the boundary conditions written as

$$\frac{\tilde{n}^1_\alpha-\tilde{n}^0_\alpha}{h}=\frac{\tilde{n}^1_{DT}-\tilde{n}^0_{DT}}{h}=\frac{\tilde{E}^1-\tilde{E}^0}{h}=0 \tag{17}$$

$$\tilde{n}^N_\alpha = v_\alpha+\tilde{d}_\alpha,\quad \tilde{n}^N_{DT}=v_{DT}+\tilde{d}_{DT},\quad \tilde{E}^N=v_E+\tilde{d}_E \tag{18}$$

The target system is chosen as

$$\dot{\tilde{w}}^i = D\frac{\tilde{w}^{i+1}-2\tilde{w}^i+\tilde{w}^{i-1}}{h^2}+\frac{1}{ih}D\frac{\tilde{w}^{i+1}-\tilde{w}^i}{h}-C_w\tilde{w}^i + \left(v_{fuel}+\tilde{d}_{fuel}\right)\Omega^i_{fuel}+\left(v_{aux}+\tilde{d}_{aux}\right)\Omega^i_{aux} \tag{19}$$

$$\dot{\tilde{m}}^i = D\frac{\tilde{m}^{i+1}-2\tilde{m}^i+\tilde{m}^{i-1}}{h^2}+\frac{1}{ih}D\frac{\tilde{m}^{i+1}-\tilde{m}^i}{h}-C_m\tilde{m}^i + \left(v_{fuel}+\tilde{d}_{fuel}\right)B^i_{fuel}+\left(v_{aux}+\tilde{d}_{aux}\right)B^i_{aux} \tag{20}$$

$$\dot{\tilde{f}}^i = D\frac{\tilde{f}^{i+1}-2\tilde{f}^i+\tilde{f}^{i-1}}{h^2}+\frac{1}{ih}D\frac{\tilde{f}^{i+1}-\tilde{f}^i}{h}-C_f\tilde{f}^i + \left(v_{fuel}+\tilde{d}_{fuel}\right)A^i_{fuel}+\left(v_{aux}+\tilde{d}_{aux}\right)A^i_{aux} \tag{21}$$

where $C_w, C_m, C_f > 0$ and

$$\Omega^i_{fuel}=-\sum_{k=1}^{i-1}\frac{\partial\omega^{i-1}}{\partial\tilde{n}^k_{DT}}\hat{S}^k_{DT},\qquad \Omega^i_{aux}=-\sum_{k=1}^{i-1}\frac{\partial\omega^{i-1}}{\partial\tilde{E}^k}\hat{P}^k_{aux}$$

$$B^i_{fuel}=\hat{S}^i_{DT}-\sum_{k=1}^{i-1}\frac{\partial\beta^{i-1}}{\partial\tilde{n}^k_{DT}}\hat{S}^k_{DT}\qquad B^i_{aux}=-\sum_{k=1}^{i-1}\frac{\partial\beta^{i-1}}{\partial\tilde{E}^k}\hat{P}^k_{aux}$$

$$A^i_{fuel}=-\sum_{k=1}^{i-1}\frac{\partial\alpha^{i-1}}{\partial\tilde{n}^k_{DT}}\hat{S}^k_{DT}\qquad A^i_{aux}=\hat{P}^i_{aux}-\sum_{k=1}^{i-1}\frac{\partial\alpha^{i-1}}{\partial\tilde{E}^k}\hat{P}^k_{aux}$$

ω, β, and α are backstepping transformations of the form

$$\tilde{w}^i=\tilde{n}^i_\alpha-\omega^{i-1}(\tilde{E}^0,\ldots,\tilde{E}^{i-1},\tilde{n}^0_{DT},\ldots,\tilde{n}^{i-1}_{DT},\tilde{n}^0_\alpha,\ldots,\tilde{n}^{i-1}_\alpha)$$
$$\tilde{m}^i=\tilde{n}^i_{DT}-\beta^{i-1}(\tilde{E}^0,\ldots,\tilde{E}^{i-1},\tilde{n}^0_{DT},\ldots,\tilde{n}^{i-1}_{DT},\tilde{n}^0_\alpha,\ldots,\tilde{n}^{i-1}_\alpha)$$
$$\tilde{f}^i=\tilde{E}^i-\alpha^{i-1}(\tilde{E}^0,\ldots,\tilde{E}^{i-1},\tilde{n}^0_{DT},\ldots,\tilde{n}^{i-1}_{DT},\tilde{n}^0_\alpha,\ldots,\tilde{n}^{i-1}_\alpha)$$

The boundary conditions of the target system are chosen as

$$\frac{\tilde{w}_1-\tilde{w}_0}{h}=\frac{\tilde{m}^1-\tilde{m}^0}{h}=\frac{\tilde{f}^1-\tilde{f}^0}{h}=0 \tag{22}$$

$$\tilde{w}^N=\tilde{d}_\alpha,\quad \tilde{m}^N=\tilde{d}_{DT},\quad \tilde{f}^N=\tilde{d}_E \tag{23}$$

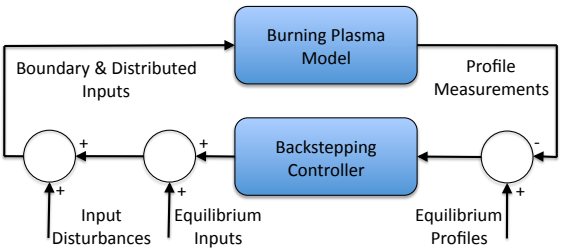

Fig. 3: Block diagram of simulation process.

The target system is chosen to maintain the parabolic character of the partial differential equation, remove the problematic nonlinear terms, and facilitate the combined use of distributed feedback and backstepping boundary feedback. By subtracting (19) from (14), (20) from (15), and (21) from (16), the expressions $\dot{\omega}^{i-1}=\dot{\tilde{n}}^i_\alpha-\dot{\tilde{w}}^i$, $\dot{\beta}^{i-1}=\dot{\tilde{n}}^i_{DT}-\dot{\tilde{m}}^i$, and $\dot{\alpha}^{i-1}=\dot{\tilde{E}}^i-\dot{\tilde{f}}^i$ are obtained, which can be put in terms of $\omega^{k-1}=\tilde{n}^k_\alpha-\tilde{w}^k$, $\beta^{k-1}=\tilde{n}^k_{DT}-\tilde{m}^k$, and $\alpha^{k-1}=\tilde{E}^k-\tilde{f}^k$, for $k=i-1,i,i+1$ and rearranged to obtain

$$\omega^i=\frac{1}{D+D/i}\left[\left(2D+\frac{D}{i}+C_wh^2\right)\omega^{i-1}-D\omega^{i-2} -h^2C_w\tilde{n}^i_\alpha+h^2\dot{\omega}^{i-1}+h^2\left(v_{fuel}+\tilde{d}_{fuel}\right)\Omega^i_{fuel} +h^2\left(v_{aux}+\tilde{d}_{aux}\right)\Omega^i_{aux}-h^2\tilde{S}^i_\alpha\right] \tag{24}$$

$$\beta^i=\frac{1}{D+D/i}\left[\left(2D+\frac{D}{i}+C_mh^2\right)\beta^{i-1}-D\beta^{i-2} -h^2C_m\tilde{n}^i_{DT}+h^2\dot{\beta}^{i-1}+h^2\left(v_{fuel}+\tilde{d}_{fuel}\right)B^i_{fuel}+2h^2\tilde{S}^i_\alpha -h^2\left(v_{fuel}+\tilde{d}_{fuel}\right)\hat{S}^i_{DT}+h^2\left(v_{aux}+\tilde{d}_{aux}\right)B^i_{aux}\right] \tag{25}$$

$$\alpha^i=\frac{1}{D+D/i}\left[\left(2D+\frac{D}{i}+C_fh^2\right)\alpha^{i-1}-D\alpha^{i-2}-h^2C_f\tilde{E}^i +h^2\dot{\alpha}^{i-1}-h^2Q_\alpha\tilde{S}^i_\alpha+h^2\tilde{P}^i_{rad}-h^2\left(v_{aux}+\tilde{d}_{aux}\right)\hat{P}^i_{aux} +h^2\left(v_{fuel}+\tilde{d}_{fuel}\right)A^i_{fuel}+h^2\left(v_{aux}+\tilde{d}_{aux}\right)A^i_{aux}\right] \tag{26}$$

where $\omega^0=\beta^0=\alpha^0=0$ and $\dot{x}^{i-1}$ (for $x\in\{\omega,\beta,\alpha\}$) is

$$\dot{x}^{i-1}=\sum_{k=1}^{i-1}\frac{\partial x^{i-1}}{\partial\tilde{n}^k_{DT}}\dot{\tilde{n}}^k_{DT}+\sum_{k=1}^{i-1}\frac{\partial x^{i-1}}{\partial\tilde{E}^k}\dot{\tilde{E}}^k+\sum_{k=1}^{i-1}\frac{\partial x^{i-1}}{\partial\tilde{n}^k_\alpha}\dot{\tilde{n}}^k_\alpha \tag{27}$$

Through its dependence on $\dot{\tilde{n}}_{DT}$, $\dot{\tilde{E}}$, and $\dot{\tilde{n}}_\alpha$, expression (27) depends on the to-be-designed control laws v_{fuel} and v_{aux}, which is not in general spatially causal, violating the strict-feedback structure required for backstepping. It also depends on the unknown terms $\tilde{d}_{fuel}$ and $\tilde{d}_{aux}$. However, by the choice of target system, the terms involving Ω^i_{fuel}, Ω^i_{aux}, B^i_{fuel}, B^i_{aux}, A^i_{fuel}, and A^i_{aux} remove the undesirable terms from the expressions (24), (25), and (26), i.e.,

$$\omega^i=\frac{1}{D+D/i}\left[\left(2D+\frac{D}{i}+C_wh^2\right)\omega^{i-1}-D\omega^{i-2} -h^2C_w\tilde{n}^i_\alpha+h^2\dot{\omega}^{i-1}_{strict}-h^2\tilde{S}^i_\alpha\right]$$

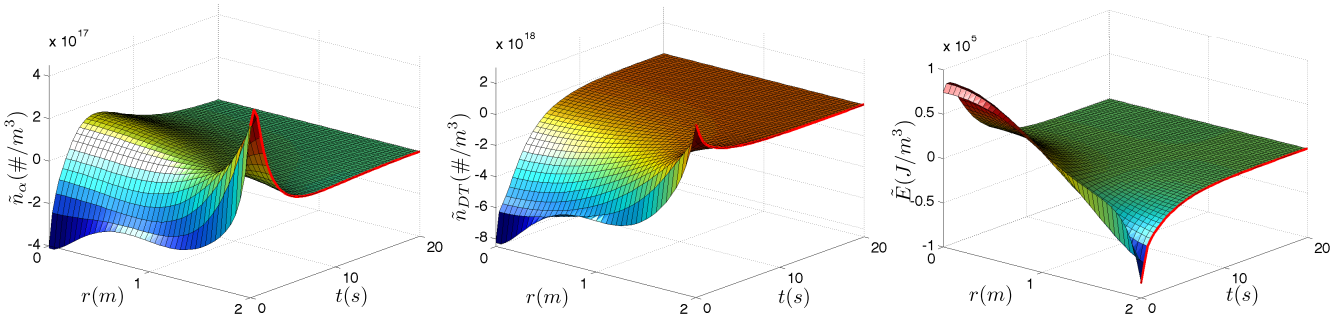

(a) Boundary feedback only.

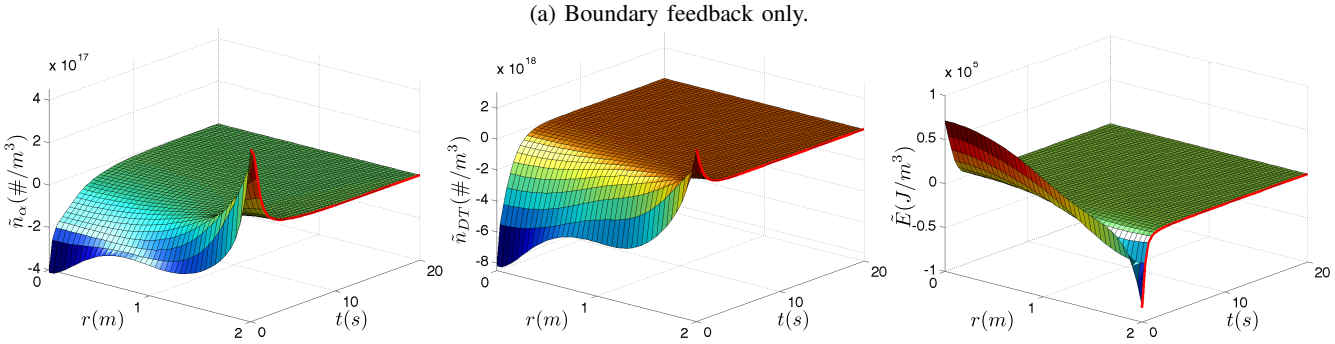

(b) Simultaneous boundary and distributed feedback.

Fig. 4: Profile error evolution with boundary feedback only (a) and with both boundary and distributed feedback (b). Solid red lines indicate the boundary actuation.

$$\beta^i = \frac{1}{D+D/i}\left[\left(2D+\frac{D}{i}+C_m h^2\right)\beta^{i-1} - D\beta^{i-2} - h^2 C_m \tilde{n}^i_{DT} + h^2\dot{\beta}^{i-1}_{strict} + 2h^2\tilde{S}^i_\alpha\right]$$

$$\alpha^i = \frac{1}{D+D/i}\left[\left(2D+\frac{D}{i}+C_f h^2\right)\alpha^{i-1} - D\alpha^{i-2} - h^2 C_f \tilde{E}^i + h^2\dot{\alpha}^{i-1}_{strict} - h^2 Q_\alpha \tilde{S}^i_\alpha + h^2\tilde{P}^i_{rad}\right]$$

where the strict feedback terms $\dot{x}^{i-1}_{strict}$, (for $x \in \{\omega, \beta, \alpha\}$) are

$$\dot{x}^{i-1}_{strict} = \sum_{k=1}^{i-1}\frac{\partial x^{i-1}}{\partial \tilde{n}^k_{DT}}\left[D\frac{\tilde{n}^{k+1}_{DT} - 2\tilde{n}^k_{DT} + \tilde{n}^{k-1}_{DT}}{h^2} + \frac{D}{ih}\frac{\tilde{n}^{k+1}_{DT} - \tilde{n}^k_{DT}}{h} - 2\tilde{S}^k_\alpha\right] + \sum_{k=1}^{i-1}\frac{\partial x^{i-1}}{\partial \tilde{n}^k_\alpha}\dot{\tilde{n}}^k_\alpha + \sum_{k=1}^{i-1}\frac{\partial x^{i-1}}{\partial \tilde{E}^k}\left[Q_\alpha\tilde{S}^k_\alpha - \tilde{P}^k_{rad} + D\frac{\tilde{E}^{k+1} - 2\tilde{E}^k + \tilde{E}^{k-1}}{h^2} + \frac{D}{ih}\frac{\tilde{E}^{k+1} - \tilde{E}^k}{h}\right] \quad (28)$$

Subtracting the boundary conditions in (23) from (18), the boundary control laws can be defined as

$$v_\alpha = \omega^{N-1}, \quad v_{DT} = \beta^{N-1}, \quad v_E = \alpha^{N-1} \quad (29)$$

The distributed control laws v_{fuel} and v_{aux}, and the disturbance estimation update laws are designed by considering the control Lyapunov function

$$V = \frac{1}{2}\sum_{i=1}^{N-1} Q^i_w\left(\tilde{w}^i\right)^2 + \frac{1}{2}\sum_{i=1}^{N-1} Q^i_m\left(\tilde{m}^i\right)^2 + \frac{1}{2}\sum_{i=1}^{N-1} Q^i_f\left(\tilde{f}^i\right)^2 + \frac{\tilde{d}^2_\alpha}{2k_\alpha} + \frac{\tilde{d}^2_{DT}}{2k_{DT}} + \frac{\tilde{d}^2_E}{2k_E} + \frac{\tilde{d}^2_{fuel}}{2k_{fuel}} + \frac{\tilde{d}^2_{aux}}{2k_{aux}}$$

where Q^i_w, Q^i_m, Q^i_f for $i \in [1, N-1]$ are positive definite weights, and k_α, k_{DT}, k_E, k_{fuel}, and k_{aux} are positive constants. Noting the equations (19), (20), and (21), and the boundary conditions (22) and (23), $\dot{V}$ can be written as

$$\dot{V} = -W^T A_w W - M^T A_m M - F^T A_f F + v_{fuel}\Phi_{fuel} + v_{aux}\Phi_{aux} + \tilde{d}_{aux}\left[\Phi_{aux} + \frac{\dot{\tilde{d}}_{aux}}{k_{aux}}\right] + \tilde{d}_\alpha\left[B_w + \frac{\dot{\tilde{d}}_\alpha}{k_\alpha}\right] + \tilde{d}_E\left[B_f + \frac{\dot{\tilde{d}}_E}{k_E}\right] + \tilde{d}_{fuel}\left[\Phi_{fuel} + \frac{\dot{\tilde{d}}_{fuel}}{k_{fuel}}\right] + \tilde{d}_{DT}\left[B_m + \frac{\dot{\tilde{d}}_{DT}}{k_{DT}}\right] \quad (30)$$

where $W = [w^1, ..., w^{N-1}]^T$, $M = [m^1, ..., m^{N-1}]^T$, $F = [f^1, ..., f^{N-1}]^T$ are transformed measurements, and $B_k = Q^{N-1}_k \frac{D}{h^2}\left(1 + \frac{1}{N-1}\right)\tilde{k}^{N-1}$ (for $k \in \{w, m, f\}$). For $D > 0$, the matrices A_k (for $k \in \{w, m, f\}$) are positive definite. The nonlinear functions Φ_{fuel} and Φ_{aux} are

$$\Phi_{fuel} = \sum_{i=1}^{N-1} Q^i_w \tilde{w}^i \Omega^i_{fuel} + \sum_{i=1}^{N-1} Q^i_m \tilde{m}^i A^i_{fuel} + \sum_{i=1}^{N-1} Q^i_f \tilde{f}^i B^i_{fuel},$$

$$\Phi_{aux} = \sum_{i=1}^{N-1} Q^i_w \tilde{w}^i \Omega^i_{aux} + \sum_{i=1}^{N-1} Q^i_m \tilde{m}^i A^i_{aux} + \sum_{i=1}^{N-1} Q^i_f \tilde{f}^i B^i_{aux},$$

We take the control laws and update laws

$$v_{fuel} = -C_{fuel}\Phi_{fuel}, \quad v_{aux} = -C_{aux}\Phi_{aux}, \quad (31)$$

$$\dot{\tilde{d}}_{fuel} = k_{fuel}\Phi_{fuel}, \quad \dot{\tilde{d}}_{aux} = k_{aux}\Phi_{aux}, \quad (32)$$

$$\dot{\tilde{d}}_\alpha = k_\alpha B_w, \quad \dot{\tilde{d}}_{DT} = k_{DT} B_m, \quad \dot{\tilde{d}}_E = k_E B_f \quad (33)$$

where $C_{fuel} \geq 0$ and $C_{aux} \geq 0$, which, assuming constant disturbances, reduces (30) to

$$\dot{V} = -W^T A_w W - M^T A_m M - F^T A_f F - C_{fuel}\Phi^2_{fuel} - C_{aux}\Phi^2_{aux}$$

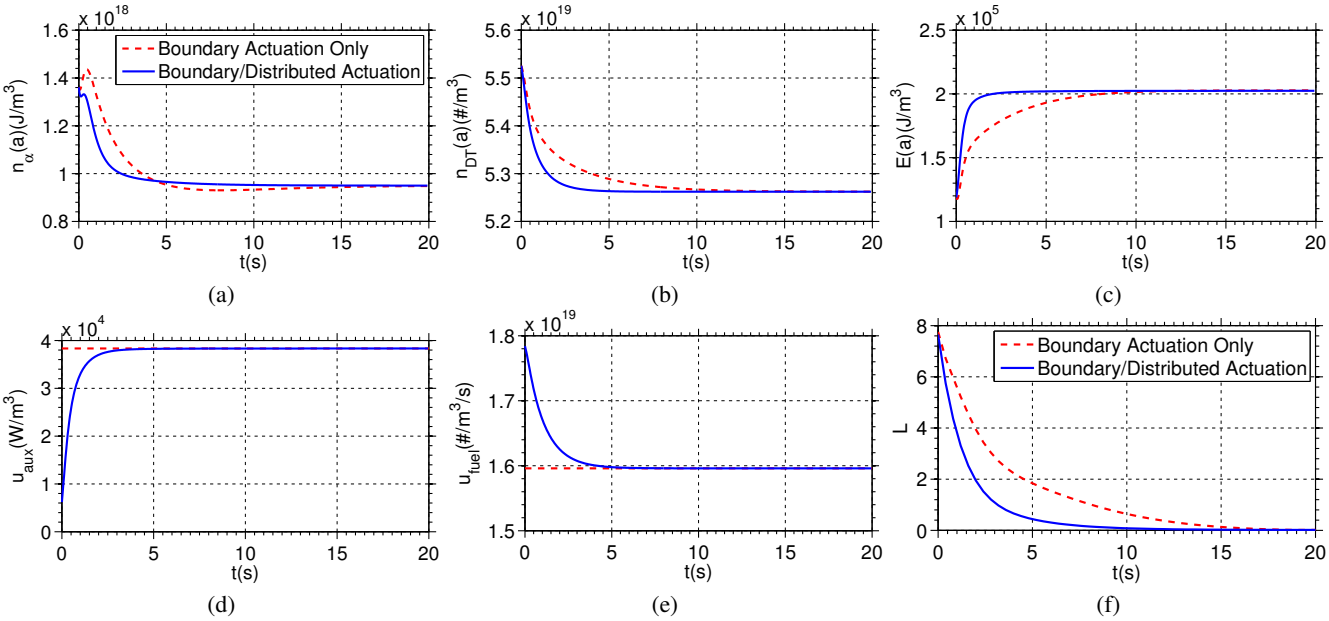

Fig. 5: Boundary actuation (a-c), distributed actuation (d,e), and l_2 norm of profile error (f), comparing a simulation with boundary actuation only (red, dashed) to one employing simultaneous boundary and distributed actuation.

Since A_w, A_m, and A_f are positive definite, we have that $\dot{V} \leq 0$. Since $V \geq 0$ and $\dot{V}$ is bounded, the conditions of Barbalat's lemma are satisfied, and we have that $\dot{V} \to 0$. This implies that $\tilde{w}$, $\tilde{m}$, and $\tilde{f}$ are driven to zero, guaranteeing asymptotic stability of the target system, and, consequently, $\tilde{n}_\alpha$, $\tilde{n}_{DT}$, and $\tilde{E}$. The control strategy is summarized in Figure 3. A set of equilibrium profiles is regulated by the backstepping controller through actuation of the ion densities and energy at the plasma edge, as well as the magnitudes of the distributed heating and fueling actuators to achieve the desired profiles.

V. Simulation Results

In the following, the discretized burning plasma system was simulated using an implicit finite difference scheme with $N_{sim} = 50$, and the time step chosen to achieve suitable accuracy. The results shown are for an open-loop unstable equilibrium described by $D_E = 0.4$, $D_{DT} = 0.2$, $D_\alpha = 0.13$, $\bar{u}_{aux} = 3.8 \times 10^4$, $\bar{u}_{fuel} = 1.6 \times 10^{19}$, $\bar{u}_\alpha = 9.5 \times 10^{17}$, $\bar{u}_{DT} = 5.3 \times 10^{19}$, and $\bar{u}_E = 2.0 \times 10^5$. As a first test, two closed loop simulations were run: one with boundary actuation only (i.e., $C_{fuel} = C_{aux} = 0$), and one with simultaneous boundary and distributed actuation ($Q_w^i = 10^{-36}$, $Q_m^i = 10^{-38}$, and $Q_f^i = 10^{-10}$ for $1, \ldots, i, \ldots N-1$, $C_{fuel} = 0.125 \times 10^{38}$, $C_{aux} = 0.1 \times 10^{10}$). Neither simulation included disturbances or disturbance estimation. In both cases, the controller was designed using $N_{control} = 3$, i.e., utilizing two measurement points inside the plasma core, and $C_w = C_m = C_f = 0.15$. Figure 4 shows the resulting profile evolutions. In both cases, the nonlinear controller was able to stabilize the desired equilibrium, however, the use of distributed actuation improved the response by adding more control authority in the interior of the plasma. Figure 5 (a)-(e) compares the boundary and distributed actuation during the two simulations. By including distributed actuation, the amount of boundary actuation needed to stabilize the system was reduced. The weighted norm of the profile error

$$L = \sqrt{\sum_{i=1}^{N-1} \left[\left(10^{-5}\tilde{E}^i\right)^2 + \left(10^{-18}\tilde{n}_\alpha^i\right)^2 + \left(10^{-19}\tilde{n}_{DT}^i\right)^2 \right] h}$$

during both simulations is compared in Figure 5 (f), showing that the profile error was driven to zero more quickly when distributed actuation was added. To test disturbance rejection, a second set of simulations were run with input disturbances $d_\alpha = -0.2\bar{u}_\alpha$, $d_{DT} = -0.2\bar{u}_{DT}$, $d_E = 0.2\bar{u}_E$, $d_{fuel} = -0.2\bar{u}_{fuel}$, and $d_{aux} = 0.2\bar{u}_{aux}$. The first simulation was run without online disturbance estimation, while estimation was active in the second ($k_\alpha = 1.2 \times 10^{36}$, $k_{DT} = 1.5 \times 10^{38}$, $k_E = 1.2 \times 10^{10}$, $k_{fuel} = 0.03 \times 10^{10}$, and $k_{aux} = 0.06 \times 10^{38}$). Figures (6) (a)-(e) compare the realized (controlled actuation + input disturbance) values of $n_\alpha(a) = u_\alpha + d_\alpha$, $n_{DT}(a) = u_{DT} + d_{DT}$, $E(a) = u_E + d_E$, distributed heating $u_{aux} + d_{aux}$, and distributed fueling $u_{fuel} + d_{fuel}$, respectively, to the values associated with the desired equilibrium. Figure 6 (f) compares the weighted norm L for both cases. In the first simulation, the system was stabilized by the feedback controller and the realized actuators converged to constant values, however, without estimation, a steady-state profile error developed, as made clear in Figure 6 (f). Through online estimation of the disturbances in the second simulation, the controller was able to account for the disturbances and drive the profile error to zero. Indeed, the realized actuators converged to the reference values associated with the desired equilibrium. Figure 7 compares the initial and final error profiles obtained in the two simulations. The effect of input disturbances is removed at steady-state when disturbance estimation is active.

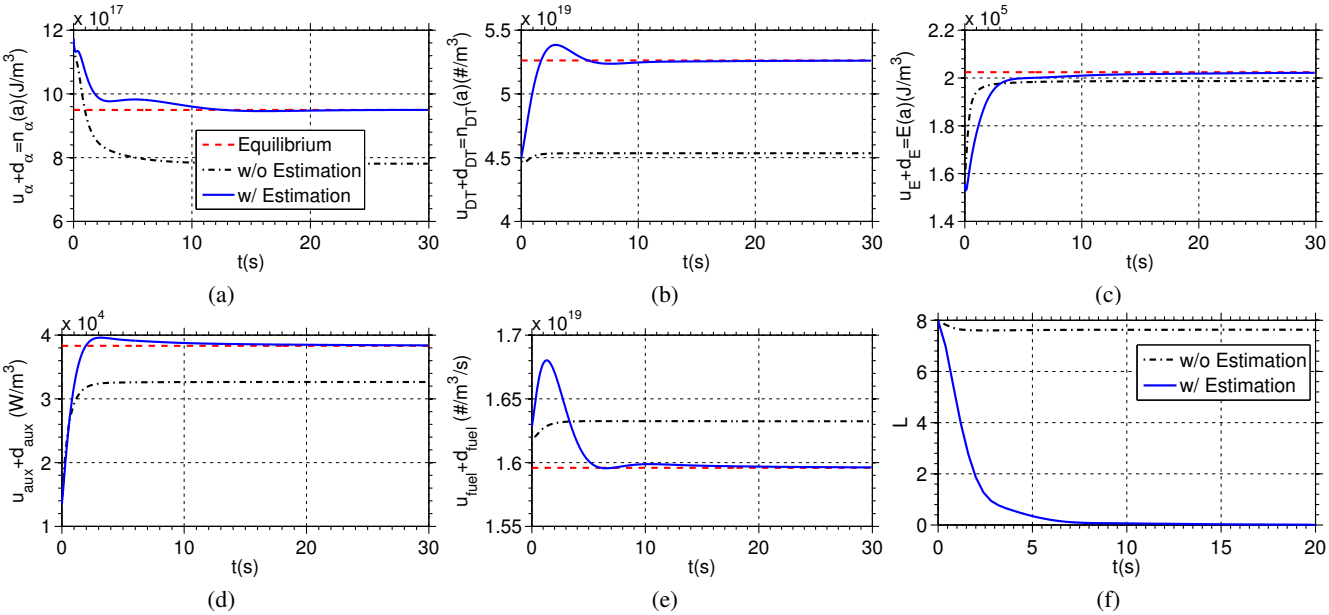

Fig. 6: Realized (controlled input + input disturbance) boundary actuation (a-c), distributed actuation (d,e), and weighted norm of the profile error (f) during simulations without disturbance estimation (black, dash-dot) and with disturbance estimation (blue, solid). With disturbance estimation, the realized actuator values converge to the reference values (red, dashed), and the profile error is driven to zero.

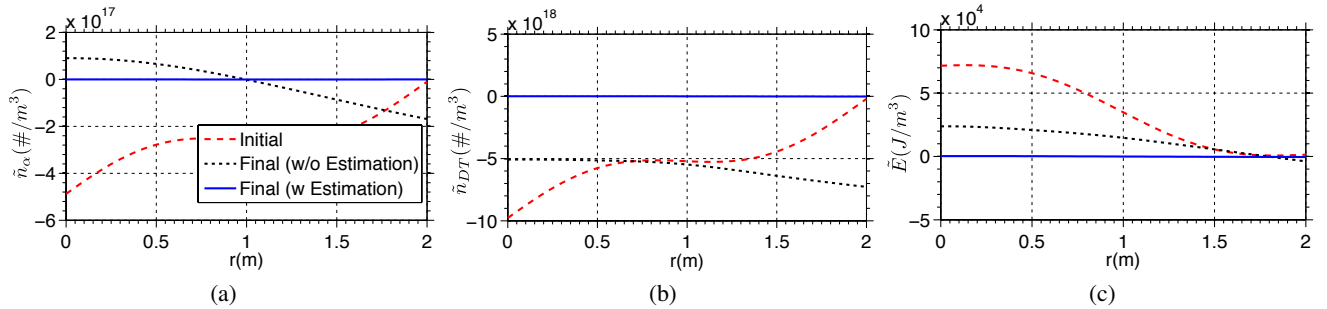

Fig. 7: Initial (red, dashed) error profiles compared to final errors with disturbance estimation (blue, solid) and without (black, dotted).

VI. Conclusions and Future Work

A nonlinear feedback controller based on backstepping that achieves asymptotic stabilization of the equilibrium kinetic profiles in a cylindrical burning plasma has been designed. The controller uses actuation of the α-particle, energy, and DT density at the plasma's edge, as well as distributed heating and fueling to stabilize the profiles. Simulations show that a controller using a coarse discretization can successfully control the profiles. While feasibility of controlling kinetic profiles in a burning plasma using a combination of distributed and boundary feedback has been shown, more study will be necessary to find methods for achieving the requested values of u_α, u_{DT}, and u_E through modulation of the plasma edge and scrape-off layer (SOL) using gas puffing, gas pumping, or impurity injection.

References

[1] M. Boyer and E. Schuster, "Adaptive Nonlinear Burn Control in Tokamak Fusion Reactors," in *Proc. of the American Control Conf.*, 2012.

[2] M. D. Boyer and E. Schuster, "Zero-dimensional Nonlinear Burn Control Using Isotopic Fuel Tailoring for Thermal Excursions," in *Proc. of the IEEE Multi-conf. on Systems and Control*, IEEE, 2011.

[3] E. Schuster, M. Krstic, and G. Tynan, "Burn Control in Fusion Reactors Via Nonlinear Stabilization Techniques," *Fusion Sci. and Tech.*, vol. 43, pp. 18–37, 2003.

[4] V. Fuchs, M. M. Shoucri, G. Thibaudeau, L. Harten, and A. Bers, "High-Q Thermally Stable Operation of a Tokamak Reactor," *IEEE Transactions on Plasma Science*, vol. PS-11, no. 1, pp. 4–18, 1983.

[5] M. A. Firestone and C. E. Kessel, "Plasma Kinetic Control in a Tokamak," *Plasma Physics*, vol. 19, no. I, pp. 29 – 41, 1991.

[6] G. Miley and V. Varadarajan, "On self-tuning control of tokamak thermokinetics," *Fusion Technology*, vol. 22, p. 425, 1992.

[7] M. A. Firestone, J. W. Morrow-Jones, and T. K. Mau, "Comprehensive Feedback Control of a Tokamak Fusion Reactor," *Fusion Tech.*, vol. 32, pp. 390–403, 1997.

[8] M. A. Firestone, J. W. Morrow-Jones, and T. K. Mau, "Developing Integrated Tokamak Dynamics Models for Next Generation Machine Control," *Fusion Tech.*, vol. 32, pp. 526–544, 1997.

[9] E. Schuster and M. Krstić, "Control of a non-linear PDE system arising from non-burning tokamak plasma transport dynamics," *International Journal of Control*, vol. 76, pp. 1116–1124, Jan. 2003.

[10] M. D. Boyer and E. Schuster, "Backstepping control of density and energy profiles in a burning tokamak plasma," in *Proceedings of the Conference on Decision and Control (CDC), 2011*, IEEE, 2011.

[11] L. Hively, "Special Topic Convenient Computational Forms For Maxwellian Reactivities," *Nuclear Fusion*, vol. 17, no. 4, p. 873, 1977.